ARCHIVIO ISTITUZIONALE
DELLA RICERCA

Alma Mater Studiorum Università di Bologna
Archivio istituzionale della ricerca

Solution and solid state photochromism in a family of shape persistent azobenzene tetramers functionalized with alkyloxy substituents

This is the final peer-reviewed author's accepted manuscript (postprint) of the following publication:

Published Version:
Vialetto, J., Groppi, J., La Rosa, M., Silvi, S., Credi, A., Baroncini, M. (2019). Solution and solid state photochromism in a family of shape persistent azobenzene tetramers functionalized with alkyloxy substituents. PHOTOCHEMICAL & PHOTOBIOLOGICAL SCIENCES, 18, 2281-2286 [10.1039/c9pp00022d].

Availability:
This version is available at: https://hdl.handle.net/11585/685394 since: 2019-09-16

Published:

DOI: http://doi.org/10.1039/c9pp00022d

Terms of use:

Some rights reserved. The terms and conditions for the reuse of this version of the manuscript are specified in the publishing policy. For all terms of use and more information see the publisher's website.

This item was downloaded from IRIS Università di Bologna (https://cris.unibo.it/).
When citing, please refer to the published version.

(Article begins on next page)

09 November 2026

Solution and solid state photochromism in a family of shape persistent azobenzene tetramers functionalized with alkyloxy substituents†

Received 00th January 20xx,
Accepted 00th January 20xx

DOI: 10.1039/x0xx00000x

www.rsc.org/

Jacopo Vialetto,[a,b] Jessica Groppi,[c,d] Marcello La Rosa,[c] Serena Silvi,[a] Alberto Credi [*c,d] and Massimo Baroncini [*c,d]

Shape-persistent azobenzene tetramers functionalized at the periphery with alkyloxy substituents of different length have been synthesized, and their photochemical behaviour has been investigated. Efficient *E* → *Z* photoisomerization of the azobenzene units takes place both in solution and in the solid state, a highly desirable yet uncommon property for azobenzene-type photochromic compounds. The solid state *E* → *Z* photoisomerization is accompanied by an isothermal crystal–amorphous phase transformation; successively, anisotropic crystals can be grown upon promoting the *Z* → *E* isomerization by thermal annealing of the irradiated samples. These results validate the strategy of engineering multiphotochromic architectures with a rigid star-shaped geometry to preserve the solution-based photoreactivity also in the solid state. The observed unexpected photoinduced alignment makes these materials potentially attractive for the development of photo-patternable and photo-responsive surfaces.

Introduction

Azobenzene is one of the most investigated photochromic compound due to its facile functionalization[1] and a clean, fast and reversible light-induced isomerization between two stereoisomers (*E* and *Z*) that exhibit markedly different physico-chemical properties, such as dipole moment, spectroscopic features, and molecular geometry.[2] Azobenzene photochromism is indeed of interest for information storage,[3,4] optoelectronic devices,[5] nanomachines,[6,7,8] control of chemical reactivity,[9] responsive surfaces[10] and materials,[11,12,13] energy conversion[14] and photo-pharmacology.[15,16]

In view of these applications, a huge number of studies on azobenzene photoreactivity have been carried out; most of them, however, are concerned with the photoisomerization of azobenzene in solution, polymers,[17] liquid crystals,[18] and inside porous materials.[19] Conversely, the photoinduced isomerization of azobenzene species in the solid crystalline state continues to be a considerable challenge,[20,21] presumably because of the relatively large free volume change associated with the conversion between the *E* and *Z* stereoisomers. Recently we described a new class of multiphotochromic materials characterized by a rigid tetrahedral three-dimensional arrangement of four azobenzene moieties.[22] Due to the rigid branched architecture, the molecules cannot efficiently pack together in the solid and porous crystal structures are obtained. The gained free volume and the occurrence of weak intermolecular interactions enable the photoisomerization of the azobenzene arms even in the crystalline solid state.

Building on these results, we present the synthesis and characterization of a series of three derivatives based on the same tetrahedral spatial arrangement of azobenzenes (Figure 1), functionalized with electron donating alkyloxy chains of different length. We envisaged that these peripheral substituents could enhance the dynamic properties of the molecules in the crystal, and possibly promote different arrangements by modulating the Van der Waals interactions as a function of the chain length. Here we describe the spectroscopic and photochemical properties of these new

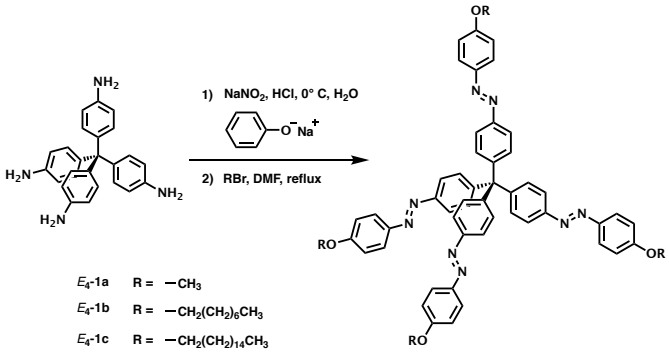

Figure 1. Synthetic scheme and structure of the investigated compounds.

[a] Dr. J. Vialetto, Dr. S. Silvi
Dipartimento di Chimica "G. Ciamician", Università di Bologna
Via Selmi 2, 40126 Bologna, Italy.
[b] Current Address: PASTEUR, Department of Chemistry, École Normale Supérieure, PSL University, Sorbonne Université, CNRS, 75005 Paris, France.
[c] Dr. J. Groppi, Dr. M. La Rosa, Prof. Dr. A. Credi, Dr. M. Baroncini
CLAN-Center for Light Activated Nanostructures
Dipartimento di Scienze e Tecnologie Agro-alimentari
Università di Bologna
Via Gobetti 101, 40129 Bologna, Italy
E-mail: alberto.credi@unibo.it, massimo.baroncini@unibo.it
[d] Dr. J. Groppi, Prof. Dr. A. Credi, Dr. M. Baroncini
Istituto ISOF-CNR
Via Gobetti 101, 40129 Bologna, Italy.

† Dedicated in memory of Prof. Ugo Mazzucato.

Electronic Supplementary Information (ESI) available: Details on the synthesis and characterization of all described compounds are available in the SI. See DOI: 10.1039/x0xx00000x

Please do not adjust margins

compounds, with particular regard to their behaviour in the solid state.

Results and discussion

Synthesis and spectroscopic analysis in solution.

Compounds E_4-**1a**–**c** (Figure 1), with their four azobenzene units in the *E* configuration and methoxy, octyloxy and hexadecyloxy substituents, respectively, were synthesized by exhaustive diazotization of tetra(4-aminophenyl)methane followed by diazo coupling with phenol to yield the intermediate tetra(4-hydroxyphenyl)methane that was then alkylated with an excess of the corresponding bromoalkane. The products were obtained in fair to good yield following a simple purification by precipitation from a concentrated acetone solution with addition of water (for details see SI).

Table 1. Photophysical and photochemical data of the investigated compounds

Compound	λ_{max} (nm) ε ($M^{-1}\cdot cm^{-1}$)[a]	$\phi_{E\rightarrow Z}$[b]	$[Z]_{365}$[c] (%)	$[Z]_{436}$[d] (%)	$k_{Z\rightarrow E}$[e] (s^{-1})
E_4-**1a**	358 nm $11.6\cdot10^4$	0.28	94	65	$1.1\cdot10^{-4}$ $1.6\cdot10^{-5}$
E_4-**1b**	361 nm $11.7\cdot10^4$	0.27	95	65	$9.6\cdot10^{-6}$
E_4-**1c**	362 nm $12.8\cdot10^4$	0.28	93	65	$3.4\cdot10^{-4}$ $5.4\cdot10^{-5}$

[a] Wavelength and molar absorption coefficient of the π-π* band maxima. [b] Quantum yield of *E* → *Z* photoisomerization upon irradiation at 365 nm. [c] Percentage of *Z* azobenzene units at the photostationary state (PSS) upon irradiation at 365 nm as determined by ^{1}H NMR. [d] Percentage of *Z* azobenzene units at the PSS upon irradiation at 436 nm. [e] Rate constant of the thermal *Z* → *E* isomerization at room temperature; two rate constants are reported when a kinetic model consisting of two consecutive first order reactions was employed to fit the experimental data.

family according to Rau's classification of substituted azobenzene.[23]

Despite the presence of long alkyloxy chains, in particular for E_4-**1c**, all investigated compounds do not show significant aggregation in CH_2Cl_2 as revealed by the perfect linear relationship between absorbance and concentration up to millimolar range (See SI). The absorption wavelength and molar coefficient of the π-π* band maximum for the different species are reported in Table 1. In the following we will describe the properties of **1a** as a representative member of the series, while noting in detail when the three compounds display a different behaviour (see SI).

Irradiation of E_4-**1a** with UV light at 365 nm causes the *E* → *Z* isomerization of the azobenzene units that is readily detected by the typical shift to higher energy and reduction in intensity of the π-π* band (Figure 2a). The fact that isosbestic points in the absorption spectra are not precisely maintained throughout the irradiation indicates that the four azobenzene units of E_4-**1a** exhibit similar but not identical photophysical and photochemical properties. This is not unexpected since photoisomerization of E_4-**1a** proceeds through the successive formation of five different stereoisomers (namely: E_4-**1a**, E_3Z_1-**1a**, E_2Z_2-**1a**, E_1Z_3-**1a** and Z_4-**1a**) which can have slightly different photophysical parameters. The percentage of total azobenzene units converted from *E* to *Z* at the photostationary state (PSS) is over 90% for all species, as determined by ^{1}H NMR analysis of solutions in deuterated dichloromethane exhaustively irradiated with light of 365 nm. The quantum yield of the *E* → *Z* photoisomerization $\phi_{E\rightarrow Z}$ at low conversion is around 0.28 for all investigated compounds, a value considerably higher than that previously reported for analogous species with alkyl substituents in place of the alkyloxy ones.

Irradiation with light of 436 nm of a solution of E_4-**1a**, previously brought at the PSS with light of 365 nm, leads to a new PSS

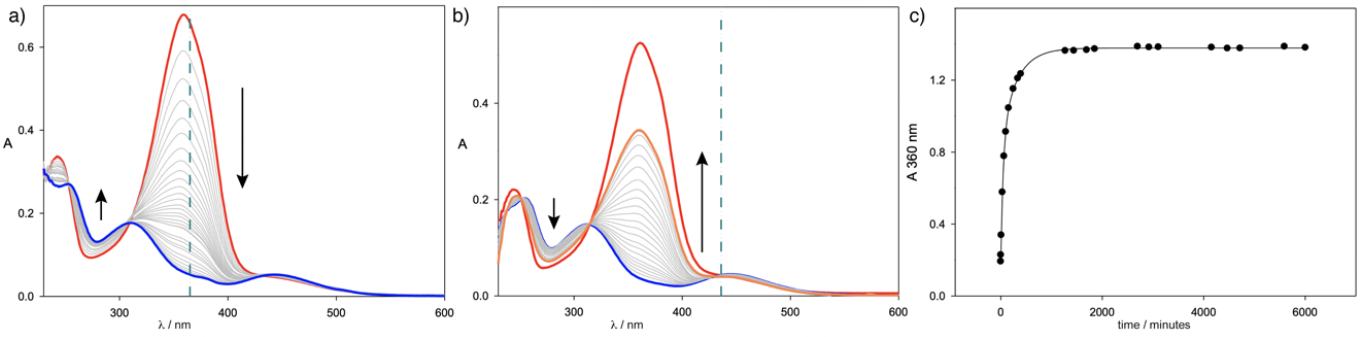

Figure 2. a) Absorption spectra of a solution of E_4-**1a** before (red trace) and after (blue trace) exhaustive irradiation at 365 nm, marked by the vertical dashed line. b) Absorption spectra of a solution of E_4-**1a** (red trace), and of E_4-**1a** exhaustively irradiated at 365 nm before (blue trace) and after (orange trace) exhaustive irradiation at 436 nm, marked by the vertical dashed line. Spectra taken at intermediate times during irradiation are shown in light grey. The direction of the spectral variations is indicated by solid black arrows. c) Time-dependent absorption changes at 360 nm upon thermal back isomerization at room temperature of a solution of E_4-**1a** subjected to previous exhaustive irradiation at 365 nm. The experimental data (black dots) are fitted with a kinetic model comprising two consecutive first order elementary reactions (grey trace).

to that of unsubstituted azobenzene, causing an increased overlap with the n-π* band. This is a typical feature of azobenzene compounds functionalized with electron donating moieties, categorized as members of the amino-azobenzene

enriched in *E* azobenzene units up to a total percentage of around 35% (Figure 2b). Alternating irradiation with light of 365 and 436 nm thus allows a clean and reversible photo-controlled switching between *Z* and *E* azobenzene-rich photostationary states. Remarkably, the thermally activated *Z* → *E* reaction that

leads from the photostationary mixture of different *Z*-containing stereoisomers (i.e., E_3Z_1-**1a**, E_2Z_2-**1a**, E_1Z_3-**1a** and Z_4-**1a**) to the single thermodynamically stable species with all azobenzene units in the *E* configuration (E_4-**1a**) is particularly sensitive to the physico-chemical inequivalence of the different interconverting stereoisomers. Indeed, upon letting a solution exhaustively irradiated at 365 nm to relax thermally at room temperature back to the all-*E* isomer, only compound **1b** shows spectral variations that can be fitted with a first order kinetic model. For compounds **1a** and **1c**, a kinetic model based on two successive first order reactions (i.e. A → B → C) has to be employed to satisfactorily fit the observed spectral changes. (Table 2 and Figure 2c) This observation reinforces the hypothesis that in **1a-c** the four azobenzene units are not fully independent, possibly because of homoconjugation effects, and reveals that the interaction between azobenzene moieties with different configurations belonging to the same molecule, while only slightly affecting the photochemical behaviour, strongly influences the rate constant of the thermal back conversion.

Solid-state photoreactivity and photoinduced phase transitions.

The photoisomerization reaction in the solid state was investigated by means of irradiation experiments carried out on dry films of E_4-**1a-c** deposited on a quartz slide by spin-coating from chloroform solutions. The quality and homogeneity of the spin-coated thin films enabled their investigation by UV-visible transmission absorption spectroscopy.

The absorption spectrum of solid thin films obtained by spin coating a solution of E_4-**1a** and a solution of E_4-**1a** previously exhaustively irradiated at 365 nm, are similar to the corresponding spectra recorded in solution. Specifically, the same typical π-π* and n-π* bands are observed, although a more distinct vibrational structure and a slight red shift of the π-π* band – that can be attributed to the rigid environment and the stronger intermolecular interactions – are seen in the solid state.[24]

Irradiation of the E_4-**1a** film at 365 nm brings about spectral changes (Figure 3a) almost identical to those found in solution, indicating efficient *E* → *Z* isomerization. From a comparison of the spectra it can be estimated that, at the PSS, about 50% of the azobenzene units are converted to the *Z* configuration. A value lower than that reached in solution with light of the same wavelength but one of the higher conversion degree observed for an azobenzene based compound in the solid state.[22]

Exposure to light of 436 nm or 289 nm of a film prepared by spin coating a solution of E_4-**1a** previously irradiated at the PSS with light of 365 nm causes *Z* → *E* photoisomerization and leads to a PSS enriched in *E*-azobenzene units (Figure 3b).

The same PSS is reached by exposure to light of 436 nm or 289 nm of a E_4-**1a** film previously irradiated with light of 365 nm (Figure 3c). The absorption spectrum recorded before any irradiation is fully restored by heating the film at 130 °C for 20 min. These observations indicate that: 1) the thermal *Z* → *E* isomerization occurs in the solid state; 2) E_4-**1a** is the thermodynamically stable form of **1a** also in the solid; 3) the photoreaction is a clean process showing no hysteresis in the thin film. Indeed, the composition reached at the PSS depends only on the irradiation wavelength and is not affected by initial differences in the stereoisomeric composition of the film (see Table 2).

Table 2. Composition at PSS (%) of thin films of the investigated compounds[a]

	λ_{irr} = 289 (nm)[b]		λ_{irr} = 365 (nm)[c]		λ_{irr} = 436 (nm)[b]		λ_{irr} = 436 (nm)[d]	
Compound	[E]	[Z]	[E]	[Z]	[E]	[Z]	[E]	[Z]
E_4-**1a**	80	20	49	51	73	27	71	29
E_4-**1b**	87	13	49	51	81	19	79	21
E_4-**1c**	87	13	50	50	74	26	80	20

[a] An experimental error of ±5% is associated with the data. [b] Composition at the PSS of thin films of E_4-**1a–c** previously exhaustively irradiated at λ_{irr}=365. [c] Composition at the PSS of thin films of E_4-**1b–c** spin coated from chloroform solutions. [d] Composition at the PSS of thin films obtained by spin coating a chloroform solutions of **1b–c** exhaustively irradiated at λ_{irr}=365.

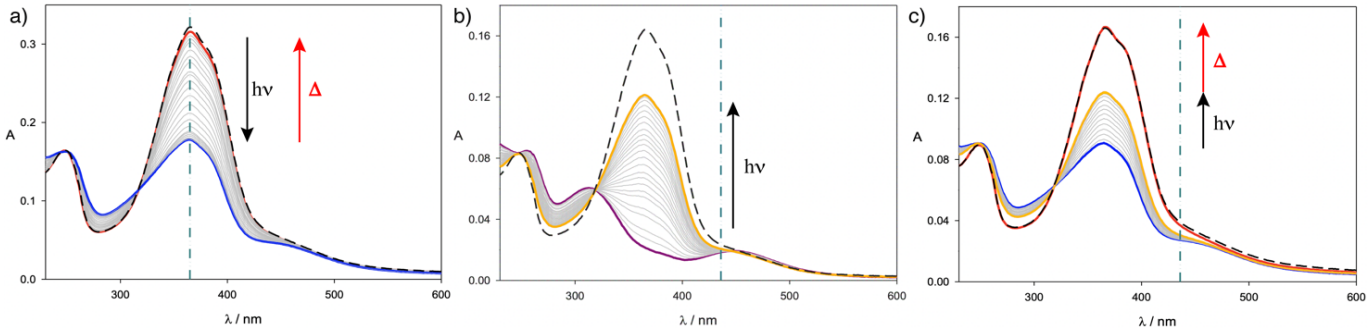

Figure 3. a) Absorption spectra of a spin coated film of E_4-**1a** before (black dashed trace) and after irradiation at 365 nm (blue trace); the red trace represents the spectra obtained after heating the irradiated film at 130 °C for 20 min. b) Absorption spectra of a spin coated film prepared from a solution of E_4-**1a** (black dashed trace) and from a solution of E_4-**1a** previously irradiated to the PSS with light of 365 nm before (magenta trace) and after exhaustive irradiation at 436 nm (orange trace). c) Absorption spectra of a spin coated film of E_4-**1a** (black dashed trace) and of a film of E_4-**1a** irradiated at 365 nm before (blue trace) and after irradiation at 436 nm (orange trace); the red trace represents the spectra obtained after heating the irradiated film at 130 °C for 20 min. Spectra taken at intermediate times during the irradiation are shown in light gray. The direction of the spectral variations of the ππ* band upon irradiation or heating are indicated respectively by black and red solid arrows. The vertical dashed lines mark the irradiation wavelength employed in the experiments.

Taken together, these experiments prove that the rigid tetrahedral arrangement effectively promotes a clean and reversible photochromism in the solid state, and that the functionalization with electron donating groups affords a higher

degree of photoconversion with respect to previously investigated compounds functionalized with alkyl peripheral substituents.[22] Instead, no significant differences are seen in the composition of the PSS due to the difference in length of the alkyloxy chain appended to the investigated compounds, suggesting that in the solid state the molecular arrangement leaves enough steric freedom to the mobile alkyloxy chains to not prejudice the photoreactivity.

To gain more insight into the effect of light on solid E_4-**1a–c**, we imaged films made by drop casting with a polarizing optical microscope. Under white light illumination the films of E_4-**1a** show a globular crystal morphology, while those of E_4-**1b** and E_4-**1c** display a sharp acicular crystal shape (Figure 4a and SI). Irrespective of the differences in the crystal habit all investigated compounds exhibit a strong optical birefringence under cross-polarized light illumination (Figure 4b and SI), confirming an ordered arrangement of the molecules in the solid that gives rise to anisotropic crystals. Upon near-UV (330–380 nm) irradiation of the crystals on a microscope slide, the crystal morphology changes (Figure 4c and SI) and the optical birefringence (Figure 4d and SI) disappears. Indeed, the crystals appear to melt and the material assumes the consistency of a viscous liquid. The observed phenomenon, common to irradiated films of all the investigated compounds, is in fact an isothermal photoinduced crystal–amorphous phase transformation taking place at ambient temperature. It is likely that the photoinduced change in the composition of the film that leads to a mixture of different stereoisomers, results in the formation of a eutectic with a melting point lower than room temperature; the photogenerated material is thus amorphous and not birefringent.[25,26]

Birefringent crystals are formed on annealing the irradiated sample of E_4-**1a** and E_4-**1b** at 130 °C for 20 min as a consequence of the $Z \rightarrow E$ thermal isomerization, in analogy to the behavior of the parent species with peripheral alkyl substituents (see SI).[22] Instead, irradiated samples of E_4-**1c** (bearing long dodecyloxy chains) upon annealing at 130 °C for 20 min (Figure 4e) display only a weak birefringence (Figure 4f) with four sharp diagonal and extinction positions 90 degree apart, readily observed by rotating the sample on the microscope stage (Figure 5).[27] This finding suggests that in the case of **1c** the solidification from the melt phase, as a consequence of the $Z \rightarrow E$ thermal isomerization, leads to a mostly amorphous phase. Such a low crystallinity can be rationalized considering that in **1c** the conformational freedom associated with the long alkyloxy chains can considerably slow down the kinetics of self-assembly of the crystalline lattice in the highly viscous melt phase, thwarting the growth of a well-arranged crystalline phase.

The observation of sharp diagonal and extinction positions in the sample, however, implies not only that some degree of crystallinity shows up on thermal annealing but also that, most unexpectedly, the crystalline regions grow anisotropically from the melt phase. As this phenomenon is detected only in films of **1c**, it can be hypothesized that the interaction of the long dodecyloxy chains with the quartz substrate or with crystalline domains enduring the photoinduced phase transition – thus able to act as crystallization seeds - favors the crystal growth

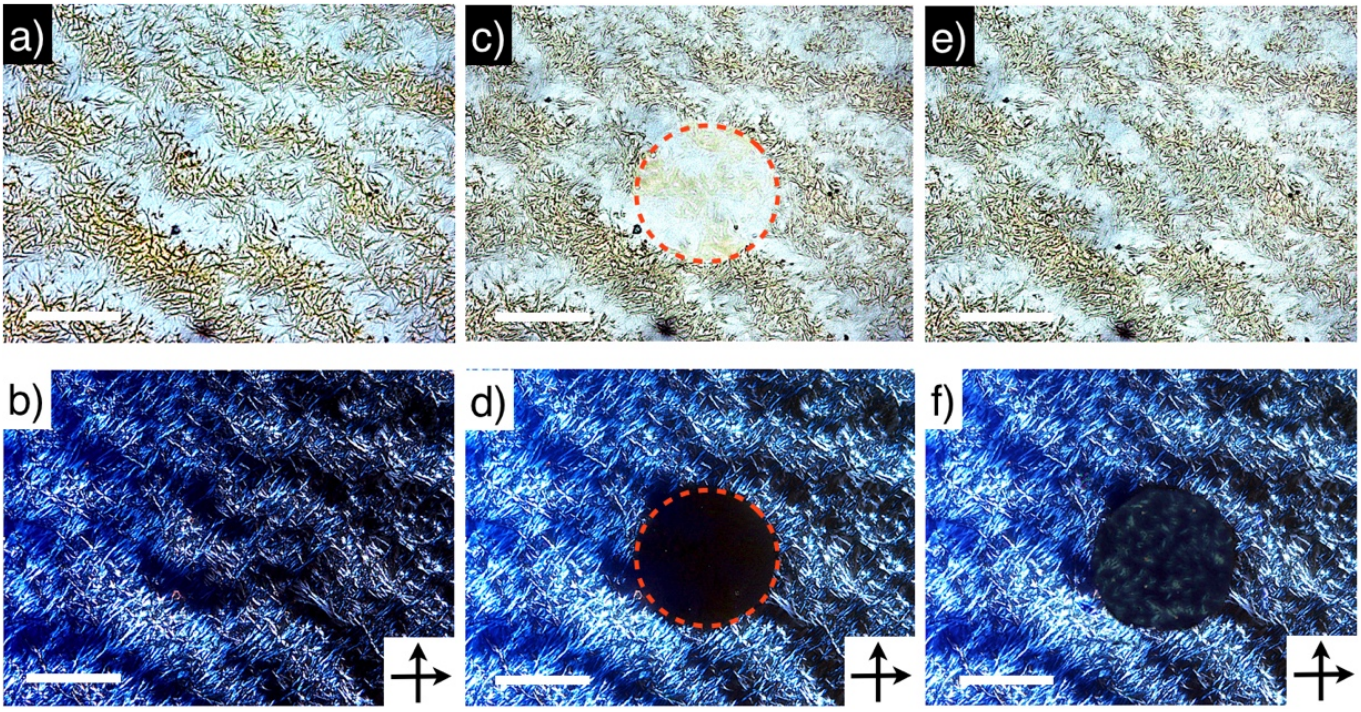

Figure 4. Polarizing optical photomicrographs of solid E_4-**1c** under bright field (top) and cross-polarized (bottom) light illumination. a, b) Before and c,d) after near-UV irradiation (Hg lamp, Nikon UV-2A filter, bandpass: 330–380 nm) in a central spot (dashed red line) for 10 min. e, f) Recrystallization of the irradiated sample is observed upon thermal annealing at 130 °C for 20 min. Scale bar, 100 µm. The white arrows in b,d) and f) represent the relative orientation of the polarizer and analyser.

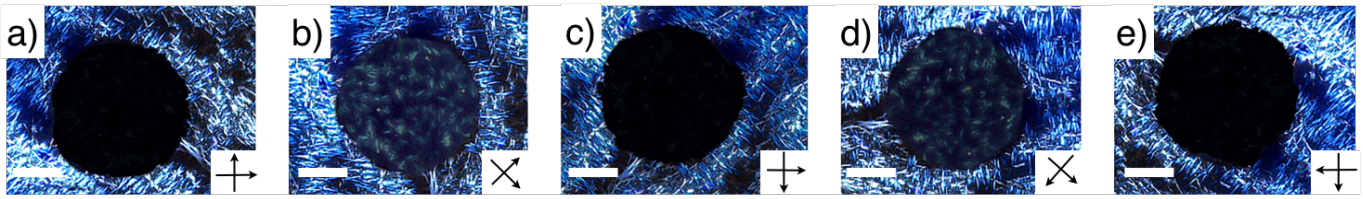

Figure 5. a) Polarizing optical photomicrographs under cross-polarized light illumination of solid E_4-**1c** irradiated in a central spot with near-UV light (Hg lamp, Nikon UV-2A filter, bandpass: 330–380 nm) and thermally annealed at 130 °C for 20 min. Scale bar, 50 μm. The black arrows represent the relative orientation of the polarizer and analyser. a, c, e) Three extinction positions and b,d) two diagonal positions are observed by rotating the sample on the microscope stage by 180 degrees.

along a preferential direction during the recrystallization from the melt phase, thus causing the alignment of the crystalline domains in the sample.[28,29] While examples of photoalignment in irradiated film of azobenzene based materials are common in the literature,[30,31] to our knowledge this is the first example of anisotropic crystal growth effected by the thermal back conversion in an azobenzene species.

Conclusions

We have reported the synthesis and photochemical investigation on a new family of compounds based on tetrahedrally arranged azobenzene units functionalized at the extremities with alkyloxy chains of different lengths. All the investigated compounds show a clean and reversible E → Z and Z → E photoisomerization in solution, while the thermally activated Z → E back reaction does not follow a simple first order kinetics, suggesting that the four azobenzene units are not fully independent. The photochromism displayed in solution is well preserved in spin coated and drop casted solid films, a very uncommon and sought-after property in photochromic materials. The efficient solid state photoreactivity of these compounds validates and generalizes our strategy of organizing photochromic moieties into rigid molecular architectures able to leave enough steric freedom to the photoactive components to enable switching in the solid state. Interestingly, the crystalline domains formed by thermal annealing previously irradiated samples of the compound with the longest peripheral chains present an unexpected long-range alignment. This phenomenon could be either due to specific interactions between the long chains and the substrate or to crystallization seeds that survive the photoinduced crystal-amorphous phase transformation and thus direct the crystal regrowth. This effect surely deserves further investigation and suggests the potential of this class of materials for the development of patternable photoactive materials and surfaces.

Experimental

Materials and Characterization Methods.
Tetra(4-aminophenyl)methane was synthesized according to previously published procedures.[32] Commercially available compounds were reagent grade quality and were used without further purification. Solvents were dried according to literature procedures. ^{1}H and ^{13}C NMR spectra were recorded at 298 K in CD_2Cl_2 with a Varian Mercury 400 MHz spectrometer equipped with a 5-mm probe. Chemical shifts were calibrated using the internal $CDCl_3$ or benzene-d6 resonances referenced to TMS. All chemical shifts are quoted using the δ scale and all coupling constants (*J*) are expressed in Hertz (Hz). Melting points were determined using a Büchi 510 series apparatus and are uncorrected.

UV-Visible Spectroscopy.
Absorption spectra were recorded at room temperature (ca. 25°C) with a Varian Cary 50Bio spectrophotometer on air equilibrated CH_2Cl_2 (Romil) solutions with concentrations ranging from $1{\cdot}10^{-5}$ to $1{\cdot}10^{-4}$ M in 1-cm quartz cells, or on thin films deposited on quartz slides by spin coating from $CHCl_3$ solutions. The experimental error on the wavelength values is ±1 nm. Polarizing optical micrographs were taken using a Nikon Eclipse 80i optical microscope.

Synthetic procedures and characterization data are reported in the ESI.

Conflicts of interest

There are no conflicts to declare.

Acknowledgements

This work was supported by the Ministero dell'Istruzione, Università e Ricerca (FARE grant n. R16S9XXKX3) and Università di Bologna.

Notes and references

1 E. Merino, *Chem. Soc. Rev.*, 2011, **40**, 3835.
2 H. M. D. Bandara and S. C.Burdette, *Chem. Soc. Rev.*, 2012, **41**, 1809.
3 F-K. Bruder, R. Hagen, T. Rölle, M-S Weiser and T. Fäcke, *Angew. Chem. Int. Ed.,* 2011, **50**, 4552.
4 S. Kawata and Y. Kawata, *Chem. Rev.*, 2000, **5**, 1777.
5 C. Raimondo, et al., *Proc. Natl Acad. Sci. USA,* 2012, **109**, 12375.
6 G. Ragazzon, M. Baroncini, S. Silvi, M. Venturi and A. Credi, *Nature Nanotech.*, 2015, **10**, 70.
7 M. Baroncini and G. Bergamini, *The Chemical Record,* 2017, **17**, 700.
8 M. Baroncini, G. Ragazzon, S. Silvi, M. Venturi and A. Credi, *Pure and Applied Chemistry,* 2015, **87**, 136.
9 R. Göstl, A. Senf and S. Hecht, *Chem. Soc. Rev.,* 2014, **43**, 1982.
10 C. Nacci, M. Baroncini, A. Credi and L. Grill, *Angew. Chem. Int. Ed.,* 2018, **130**, 15505.

11 P. Naumov, S. Chizhik, M. K. Panda, N. K. Nath and E. Boldyreva, *Chem. Rev.,* 2015, **115,** 12440.
12 Y. Hao, S. Huang, Y. Guo, L. Zhou, H. Hao, C. J. Barrett and H. Yu, *J. Mater. Chem. C,* 2019, **47**, 1044.
13 V. Fasano, M. Baroncini, M. Moffa, D. Iandolo, A. Camposeo, A. Credi and D. Pisignano, *J. Am. Chem. Soc.,* 2014, **136**, 14245.
14 L. Dong, Y. Feng, L. Wang and W. Feng, *Chem. Soc. Rev.,* 2018, **46**, 15034.
15 W. A. Velema, W. Szymanski and B. L. Feringa, *J. Am. Chem. Soc.*, 2014, **136**, 2178.
16 M. Zhu and H. Zhou, *Org. Biomol. Chem.*, 2018, **16**, 8434.
17 G. Sudesh Kumar and D. C. Neckers, *Chem. Rev.*, 1989, **89**, 1915.
18 T. Ikeda and O Tsutsumi, *Science*, 1995, **268**, 1873.
19 O. S. Bushuyev, T. Friščić and C. J. Barrett, *CrystEngComm,* 2016, **18**, 7204.
20 T. Naito, K. Horie and I. Mita, *Macromolecules,* 1991, **24**, 2907.
21 R. Evans, et al., *Nature Mater.,* 2005, **4**, 249.
22 M. Baroncini, et al., *Nature Chemistry,* 2015, **7**, 634.
23 H. Rau, *Photochromism: Molecules and Systems*, Elsevier, Amsterdam, Revised edn, 2003.
24 E. Uchida, K. Sakaki, Y. Nakamura, R. Azumi, Y. Hirai, H. Akiyama, M. Yoshida and Y. Norikane, *Chem. Eur. J.,* 2013, **19**, 17391.
25 Y. Norikane, E. Uchida, S. Tanaka, K. Fujiwara, E. Koyama, R. Azumi, H. Akiyama, H. Kihara and M. Yoshida, *Org. Lett.,* 2014, **16**, 5012.
26 M. Hoshino, E. Uchida, Y. Norikane, R. Azumi, S. Nozawa, A. Tomita, T. Sato, S.-I. Adachi and S.-Y. Koshihara, *J. Am. Chem. Soc.,* 2014, **136**, 9158.
27 P. Fesenko, C. Rolin, R. Janneck, S. P. Bommanaboyena, H. Gaethje, P. Heremans and J. Genoe, *Organic Electronics*, 2016, **37**, 100.
28 H. Minemawari, T. Yamada, H. Matsui, J. Tsutsumi, S. Haas, R. Chiba, et al., *Nature,* 2011, **475**, 364.
29 Y. Diao, et al., *Nat Mater*, 2013, **12**, 665.
30 K. Ichimura, *Chem. Rev.,* 2000, **100**, 1847.
31 A. Priimagi, M. Saccone, G. Cavallo, A. Shishido, T. Pilati, P. Metrangolo and G. Resnati, *Advanced Optical Materials,* 2012, **24**, 345.
32 F. A. Neugebauer, H. Fischer, R. Bernhardt, *Chem. Ber.* 1976, **109**, 2389.

This document is the unedited Author's version of a Submitted Work that was subsequently accepted for publication in Photochemical and Photobiological Sciences, copyright © The Royal Society of Chemistry after peer review.
To access the final edited and published work, see:
https://pubs.rsc.org/en/content/articlelanding/2019/PP/C9PP00022D